

Excitation of HF and ULF-VLF waves during charged particle beams injection in active space experiment

Nikolay V. Baranets, Yackov P. Sobolev, Yuriy Ya. Ruzhin, Hanna Rothkaehl¹⁾, Nikolay S. Erokhin²⁾, Valeriy V. Afonin²⁾, Jaroslav Vojta³⁾, and Jan Smilauer³⁾

*Institute of Terrestrial Magnetism, Ionosphere, and Radio Wave Propagation,
Russian Academy of Sciences, Troitsk, Moscow oblast, 142190 Russia*

¹⁾ *Space Research Center, Polish Academy of Sciences, 00-716 Warsaw, Poland*

²⁾ *Space Research Institute, Russian Academy of Sciences,
Profsoyuznaya ul. 84/32, Moscow, 117997 Russia*

³⁾ *Institute of Atmospheric Physics, Academy of Sciences of the Czech Republic,
14131 Prague 4, Czech Republic*

(Received: 2 September 2008 / Accepted: 1 April 2009)

Results of active space experiment with simultaneous injection of electron and xenon ion beams from the *Interkosmos-25 (IK-25)* satellite are presented. A specific feature of this experiment was that charged particles were injected in the same direction along the magnetic field lines and the particle beams simultaneously injected into the ionospheric plasma were therefore nested in one another. Results of the beam-plasma interaction for this configuration were registered by the double satellite system consisting of *IK-25* station and *Magion-3* subsatellite.

Keywords: beam-into-beam injection, ULF waves excitation, dipole antenna

1. Introduction

This paper is a continuation of work on the investigation of charged particle beams injection from the satellite *Interkosmos-25* (APEX experiment). A specific feature of the experiment carried out at the orbits 201, 202 was that the pitch-angles of electron and ion beams injection correspond to the same propagation directions along the equilibrium magnetic field \mathbf{B}_0 . Different aspects of a beam-plasma instability (BPI) for electron beam injection through the extended hollow beam of xenon ions were considered in the paper [1] for the case of orbit 202. One of the most interesting result is related to an absorption or excitation of HF waves under the electron-cyclotron resonance condition in dependence of the relation of Larmor radius of the beam electrons to a lateral wave length (with respect to \mathbf{B}_0) [2]. This feature of BPI mechanism is confirmed by the HF electric fields e_{hf} and fast electron and ion fluxes measured at *Magion-3*. Main results of the beam-plasma interaction presented in this paper are related to the excitation of HF fields in the remote region, and very low-frequency (VLF) waves in the range of lower-hybrid frequency ω_{LH} , as well as the ultra low-frequencies (ULF) $\omega \sim \omega_{ci}$ registered at *IK-25*, where $\omega_{ci} \equiv \omega_{ci}^{(H)}$ is the ion cyclotron frequency for a hydrogen plasma.

2. Equipment and spatial configuration of the injections

The ion injector was a Hall-type stationary plasma thruster (SPT) with a longitudinal acceleration of

xenon ions. The injection current varied in the range $I_{bi} \approx 2.0 - 2.6\text{A}$, and the output ion energy was up to 250eV. The electron injector was a straight-channel three-electrode electron gun (EG) operating at modulation frequencies varying from 32 Hz to 250 kHz (over a time period of 2-12s) after the first second of dc injection, with 1-s intervals between the injection cycles. The EG control electrode provided 100-% modulation of the electron beam current, $I_{be} \sim 100\text{mA}$, thereby forming separate injection micropulses with a duration of $2\mu\text{s}$. Different ionospheric parameters such as a density of unperturbed plasma n_0 and the ion plasma distribution, quasi-steady electric \mathbf{E} and magnetic field \mathbf{B} , and its variations, electric \mathbf{e}_{lf} and magnetic \mathbf{b}_{lf} component of ULF-VLF waves used in this paper are measured by the scientific instruments mounted at both satellites. Spatial field components measured in the orthogonal coordinate systems X, Y, Z and x', y', z' at the satellite and subsatellite are reduced to the new ones for the left-handed Cartesian coordinate system x, y, z with $z \parallel \mathbf{B}_0$. A more detail characteristics of the scientific payload of the mother-douther satellite system are described, for example, in the paper [3].

The system of an electron beam nested in an ion beam is axially asymmetric with respect to the magnetic field direction due to the small velocity of xenon ions ($v_{iz}/u \sim 3 \cdot 10^{-4}$), which is comparable to the velocity of the satellite ($v_{iz}/v_s \sim 1.5$) moving at an angle to the magnetic field (Fig. 1). For certain injection parameters, the generated HF oscillations can reach a saturation level (corresponding to the onset

author's e-mail: baranets@izmiran.ru

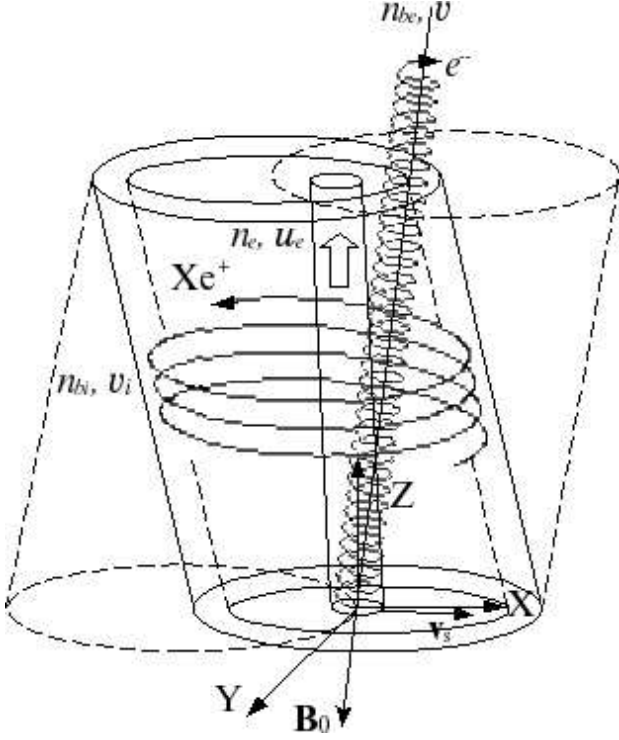


Fig. 1 Electron beam injection (e^-) directed through the hollow beam of xenon ions (Xe^+) with the beam density and velocity n_{be}, v and n_{bi}, v_i , respectively. Release of the electron flow with the density and stream velocity n_e, u_e for a compensation of the ion beam charge at the output of SPT is shown by the uparrow. Here, B_0 and v_s are the directions of the quasi-steady magnetic field and the satellite velocity in the X, Y, Z coordinate system.

of a nonlinear regime), after which the spectrum begins to extend toward lower frequencies. In this case, the hollow beam of heavy xenon ions injected at pitch angles of up to $\Delta\alpha_{pi} \simeq 60^\circ$ with a maximum flux density within the angles $\Delta\alpha_{pi} \leq 30^\circ$ will play the role of a damping layer for waves induced by the electron beam in the entire interaction region in the vicinity of the satellite. In this regard, the generation of extremely low-frequency (ELF) waves and the possibility of controlling the nonlinear interaction mechanism are of most interest [4].

3. Main features of the beam-plasma interaction

3.1. When a low-energy electron beam (~ 10 keV) is injected into the ionospheric plasma, the development of instabilities and the excitation of electromagnetic fields depend substantially on the shape and density of the beam. On the other hand, in a complex current system, the current profile depends on the energy density of the excited waves, which in turn modulate the electron beam, thereby producing a feedback in the beam-plasma system. In order to determine the main characteristics of wave excitation and

charge modulation, we assume that the electrons are injected in the presence of induced electric fields (excited over ~ 1 s), which modulate the beam in the injection region. After several gyrations of dense particle beams, electrostatic repulsion forces transform them into hollow flows with the average density n_{ba} (with $a = e, i$), determined by the expression $I_{ba} \cong 2\pi \int_{r_1}^{r_2} ev_z(r)n_{ba}(r)r dr$, where r_1 and r_2 are the minimum and maximum radii of charged particle gyration at the internal and external boundaries of the beam, $r = \sqrt{x^2 + y^2}$. The averaged flow velocity was determined as $u \equiv \langle v_z \rangle_\alpha = (1/\Delta\alpha') \int_{\Delta\alpha'} v \cos(\alpha_p + \alpha) d\alpha$, where the effective range of pitch angles is $\Delta\alpha' > \Delta\alpha_0$ ($\sim 2^\circ - 3^\circ$ and $\sim 60^\circ$ for electrons and ions, respectively, at $z = 0$). The effective range of pitch angles for electrons,

$$\Delta\alpha' \simeq \Delta\alpha_0 + \frac{\pi e}{mv\omega_{ce}} (\delta\bar{E}_x + v\delta\bar{B}_z \sin\alpha_{pe} - v\delta\bar{B}_y \cos\alpha_{pe}), \quad (1)$$

reflects the amplitude modulation of the beam by quasi-steady fields in the injection region over a time $t \sim 1$ s, where e, m are the charge and mass of electron, and ω_{ce} is the electron gyrofrequency. The upper bar, $\delta\bar{F}_{x,y,z} = \overline{F_{x,y,z}} - \bar{F}_{x,y,z}$, denotes the empirical average over the time interval $\Delta t \sim (7 \div 10)\Delta t_0$ for the any field measurements F , where Δt_0 is the duration of one telemetric frame at the *IK-25* and v is the electron velocity at $z = 0$ (at the output of the EG modulator). The smoothing of the quantities in semiempirical formula (1) is of great importance for eliminating the influence of fast fluctuations on the calculated density of the injected beam; without such a smoothing, numerical instability can arise. The fluctuation amplitudes of the longitudinal and transverse velocities of the injected particles in an equilibrium state and the thermal electron velocity in the flow were estimated using the expressions $\delta v_{\perp,z} \leq \max\{v_{\perp,z} - \langle v_{\perp,z} \rangle_\alpha\}$, and $v_{be} \sim (\delta v_z^2 + \delta v_\perp^2)^{1/2}$, respectively. These allow one to use the effective angular divergence $\Delta\psi \equiv \cos^3(\alpha_{pe} - \Delta\alpha'/2) - \cos^3(\alpha_{pe} + \Delta\alpha'/2)$ as a measure of beam heating.

3.2. An inhomogeneous electron beam in the EG chamber is produced in two stages. During short-term interaction with the driving field of the modulator $\tau\omega_m \ll 1$ ($\tau = 2 \mu s$), low-energy electrons are first modulated over velocity; then, the beam is additionally accelerated in the space between the anode and the grid modulator. The most important parameters of the electron-field interaction in EG modulator are the modulation depth ξ , the change in the field phase Θ_1 , and the efficiency with which the driving field acts on the beam electrons $G = 2 \sin(\Theta_1/2)/\Theta_1$ [5]. In the regime of modulation for the simplest case of free electron gyration in the outer space, the spectral composition of the electron current I_{be} is determined by the

expression

$$I_{be}(z, t) = I_0 + 2I_0 \sum_{n=1}^{\infty} (-1)^n J_n(nX_D(z)) \times \cos n \left[\omega_m t - \Theta_D(z) - \frac{\Theta_1}{2} \right], \quad (2)$$

where $J_n(nX_D(z))$ is the Bessel function, and $X_D(z) = \xi G \Theta_D(z)/2$ is the bunching parameter over the length z . The current I_0 is defined during the 1-s of dc-injection. The amplitudes of the harmonics of the convection current are determined by the expression $I_{be}^n(z, t) = 2I_0 J_n(nX_D(z))$. In the regime of modulation, the plasma frequency of the beam electrons ω_{be} is determined for the first harmonic of the convection current, I_{be}^1 . However, the beam particles dynamics strongly depends on the excited waves due to a plasma electromagnetic instability (EMI) and self-fields associated with the charge and current densities, thus the current appreciation $I_{be}(z, t)$ in a modulation mode is very approximate.

3.3. If one assume that the injection of heavy xenon ions does not contribute to the excitation in HF waves, then the growth rate γ of quasi-longitudinal waves with frequencies $\omega \simeq \omega_{\pm}(\theta)$ in a "cold plasma-cold beam" system can be obtained from the well known dispersion relation:

$$1 - \frac{\omega_{pe}^2}{\omega^2} \cos^2 \theta - \frac{\omega_{pe}^2 \sin^2 \theta}{\omega^2 - \omega_{ce}^2} - \frac{\omega_{be}^2 \cos^2 \theta}{(\omega - k_z u)^2} - \frac{\omega_{be}^2 \sin^2 \theta}{(\omega - k_z u)^2 - \omega_{ce}^2} = 0, \quad (3)$$

where k_z is the longitudinal component of the wave vector of waves propagating at an angle θ to the magnetic field in the Cartesian coordinate system (x, y, z) , and ω_{pe} , ω_{ce} are the electron plasma and cyclotron frequencies, respectively. The frequencies $\omega_{\pm}(\theta)$ correspond to the higher (+) and lower (-) hybrid plasma resonances. For a weak-beam approach $n_{be} \ll n_0$ and an absolute character of the instability, the solution of the Eq. (3) can be obtained for the frequencies $\omega = k_z u + n|\omega_{ce}| + \epsilon \approx \omega_{\pm}$, where $\epsilon = \delta\omega + i\gamma$ ($|\epsilon| \ll |\omega_{\pm}|$, $n = 0, \pm 1, \dots$). For moderate detunings, when $|\epsilon/(\omega_{\pm} - k_z u)| \ll 1$, or $|\epsilon(\omega_{\pm} - k_z u)| \ll |(\omega_{\pm} - k_z u)^2 - \omega_{ce}^2|$, by linearizing (3) with respect to the small parameter $|\eta| = |\epsilon/\omega_{\pm}| \ll 1$ and ignoring the terms on the order of $\sim \eta^3, \eta^4$, the dispersion equation can be reduced to the form $A\eta^2 + B\eta + C = 0$, where A, B, C are fairly complicated functions of the parameters $\omega_{pe}, \omega_{ce}, \omega_{\pm}, \omega_{be}, v$. In this case, the normalized growth rate $\gamma^H/\omega_{\pm} \equiv \text{Im} \eta$ of the excited waves is equal to

$$\text{Im} \eta = \frac{+\sqrt{|B^2 - 4AC|}}{2A}, \quad B^2 \leq 4AC. \quad (4)$$

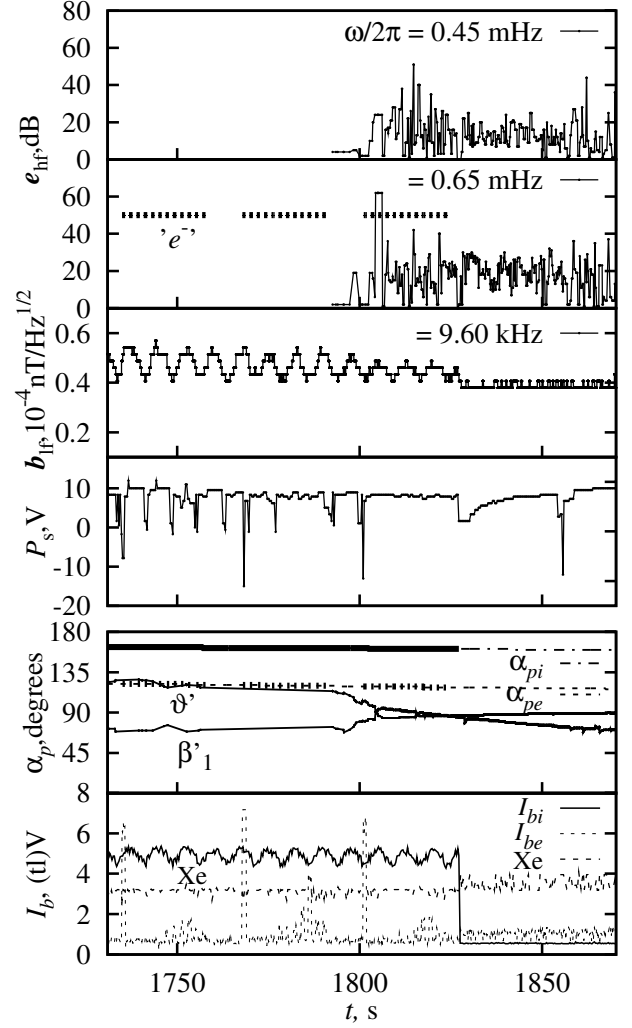


Fig. 2 Time evolution of the HF field amplitudes e_{hf} at the frequencies $\omega/2\pi = 0.45, 0.65$ mHz is registered by the PRS-S receiver at the *Magion-3*. Plots in the middle show the magnetic component of the VLF waves (9.6kHz), and potential of the satellite surface P_s . Lower plots demonstrate the pitch angles of xenon plasma and electron beam injections; the dashed lines with heavy solid segments indicate the instants of injection. The angles of β'_1 and θ' between the magnetic field and the x' -axis and the PRS-S dipole antenna, respectively, are defined in the x', y', z' -coordinate system. Records of the injection currents I_{bi} , I_{be} , and the neutral gas (Xe) release (in telemetric volts) are shown in bottom. The time t is counted from the instant 1:26:59 UT, the orbit 201 altitude is $H=1450-1715$ km.

It is known that in a hydrodynamic approach the transverse waves with $k_{\perp} = 0$ do not excited by the cold beam in which all electrons have only stream velocity u , as in previous case. However, the electromagnetic instabilities are very sensitive to an anisotropic particle velocity distribution. In this case the instability can be excited even for $\cos \theta \simeq 1$. If a distribution function can be presented in the form $\mathcal{F} = n_{be}^0 \delta(v_z - v) f_{\perp}(v_{\perp}^2)$, then for the frequency range $\omega_{ci} \ll \omega \ll \omega_{ce}$ the dispersion equation relative to the

transverse wave excitation is the following [6]

$$\frac{c^2 k^2}{\omega^2} + \frac{\omega_{pe}^2 \omega_{ce}}{\omega(\omega^2 - \omega_{ce}^2)} \cong -\frac{\omega_{be}^2}{\omega^2} \left[\frac{\omega - k_z v}{\omega - \omega_{ce} - k_z v} + \frac{k_z^2 v_{\perp}^2 / 2}{(\omega - \omega_{ce} - k_z v)^2} \right], \quad (5)$$

where n_{be}^0 , and $f_{\perp}(v_x^2 + v_y^2)$ are the unperturbed electron beam density ($\gamma \sim 0$) and two-dimensional Maxwell distribution function, respectively. It is evident from Eq.(5) that the electromagnetic wave excitation occurs in the frequency range $\omega - \omega_{ce} - k_z v \approx 0$ (normal Doppler effect, $n = 1$), i.e. for $k_z \approx -\omega_{ce}/v$. It follows that in the range of wistler mode, the backward-propagating waves are excited due to the beam-anisotropic instability. After linearizing Eq. (5) with respect to the small parameter $|\eta| = |\epsilon/\omega| \ll 1$, the dispersion equation can be reduced to the quadratic form the solution of which is analogous to Eq. (4).

4. Main results

A number of effects were observed at the satellite *IK-25* and subsatellite *Magion-3* during the electron beam injection through the flow of xenon ions. Some of them, for example, disturbances of the HF electric field presented at the top of Figure 2 are measured at *Magion-3* subsatellite on the distance $D \sim 100 - 110$ km from *IK-25* and can be excited in result of BPI development during electron beam injection. Pause in the e_{hf} recordings up to $t \cong 1792$ s is caused by the technical reasons at *Magion-3*. The magnetic component of VLF waves (9.6kHz) is registered at the *IK-25*. Figure 2 demonstrates also a strong negative bias of the satellite potential P_s in accordance with the periodic ion beam current modulations. The nature of these variations is related to an SPT-chamber accelerated ion characteristics rather than to the beam-into-beam injection features. P_s -changes are more negatively biased during a dc-injection of electrons (1-st s). The behavior of the potential P_s during electron injection is similar to that of the negative dc bias of an electrode which occurs during the injection of HF power in the plasma. The induced electromagnetic field, once generated, is sustained by electron beam injection, thereby producing a nonlinear pressure on the ambient plasma. Appearance of HF fields in the vicinity of injector can lead to an amplification (or suppressing) of low frequency waves.

It is obvious that the disturbances e_{hf} are caused by the electron beam injection, but to obtain a more detailed characteristics of the beam-plasma interaction in the remote region of ionospheric plasma, the hybrid computational algorithm was carried out at the second stage of complex data processing. The measured and calculated parameters during injection

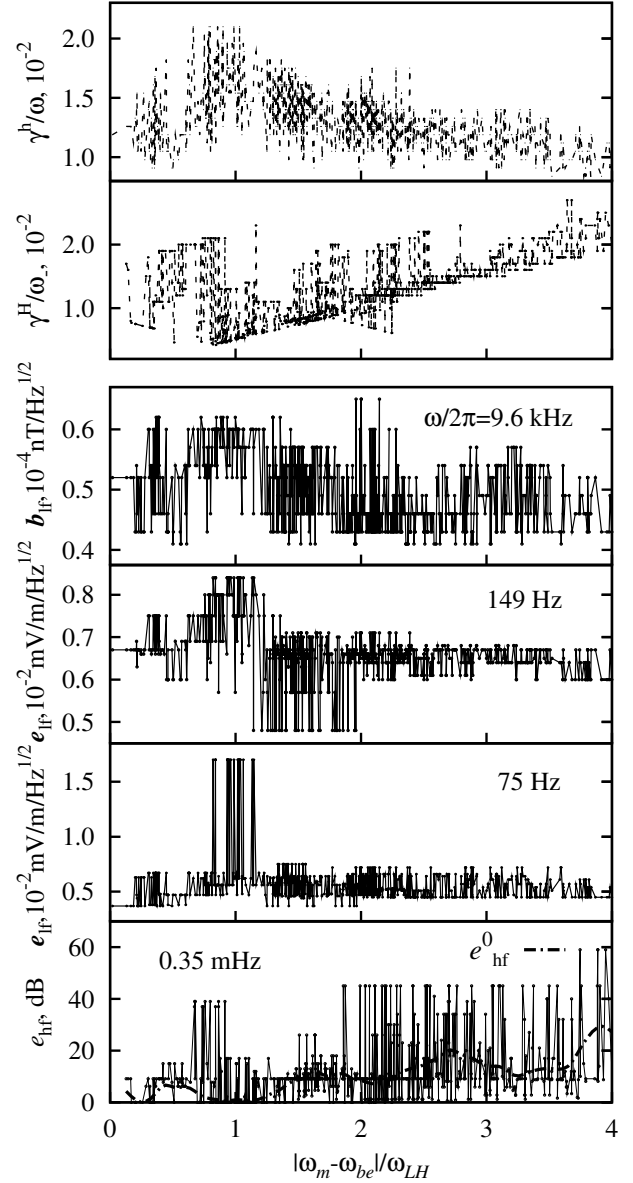


Fig. 3 Normalized growth rates of the electromagnetic instability γ^h/ω (for the $\omega \simeq \omega_{ce}/6$, $n = 1$, $\theta \simeq 0.04$) and beam-plasma instability γ^H/ω_- ($\omega \simeq \omega_-$, $n = 0$, $\theta \simeq 0.36$) at the top panels; measured amplitudes of the magnetic and electric component of ULF-VLF waves b_{if} , e_{if} (in the middle), and electric HF-fields e_{hf} (bottom) are shown versus the parameter $p = |\omega_m - \omega_{be}|/\omega_{LH}$. Dashed line on the bottom panel (Bezier spline, e_{hf}^0) indicates a trend of HF fluctuations behavior.

on, h_j and s_j respectively, were transformed (with allowance for simulations of active space experiment) into a new sequence, $h_j(t), s_j(t), p(t) \Rightarrow h_j(p), s_j(p)$, in ascending order of the parameter p . Evaluations of the growth rate of BPI and EMI processes are presented on the top of Fig. 3 as a function of the parameter $p = |\omega_m - \omega_{be}|/\omega_{LH}$, where $\omega_{LH}/2\pi \simeq 9-12$ kHz is the lower hybrid frequency ($\theta = \pi/2$). Although it is not clear which type of waves excited in the outer plasma is associated with the modulation frequency

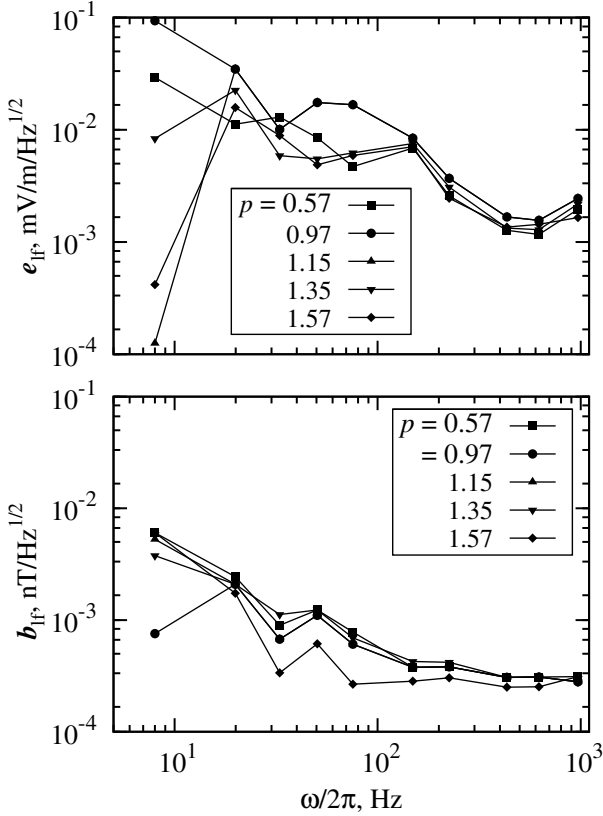


Fig. 4 Spectra of the electric and magnetic component of ELF-ULF waves, e_{if} , b_{if} , respectively, are measured at *IK-25* in the frequency range 8-969 Hz for different parameter values p (see Fig. 3.).

ω_m , we see in the Fig. 3 a reasonable relationship between three waves with frequencies ω_{be} , ω_m , and ω_{LH} . This is confirmed by a number of frequency characteristics for VLF waves and HF fluctuations registered at *IK-25* and *Magion-3*. First of all, these are the ULF-VLF waves excitation and normalized growth rate maximum γ^h/ω ($\omega \simeq \omega_{ce}/6$) observed near the parameter range $p \simeq 1$. The low-frequency limit for instability development is, in accordance with Eq. (5), $\omega \gg \omega_{ci}$, where $\omega_{ci}/2\pi \simeq 300 - 380\text{Hz}$. Thus the amplification effects for ULF waves are not caused by the hydrodynamic type instability. However, in the case of the electron plasma temperature anisotropy the kinetic instability limit ($\gamma^k \sim 0$) approaches lower frequencies $\omega \lesssim \omega_{ci}$. It is worth to note that in many cases observed in APEX experiment the spectra of ULF beam-induced waves are similar to the spectrum presented at Fig. 4 with the exception of ELF waves for $\omega \lesssim \omega_{ci}^{(Xe)}$, where $\omega_{ci}^{(Xe)}$ is the xenon ion cyclotron frequency range $\sim 14-18\text{Hz}$. In this frequency range the abrupt amplitude changes are observed as far as the triplet frequency relationship for ω_m , ω_{be} , ω_{LH} corresponds to the values $p \gtrsim 1$.

Another effects confirming the presence of three-wave coupling are observed in the remote region at *Magion-3* subsatellite. HF electric field disturbances

excited due to BPI development are shown at Fig. 3 for the frequency $\omega \simeq \omega_-$ as a function of the parameter p . Generally, in classical treatment the growth rate of longitudinal waves as a function of the beam density n_{be} in a "cold plasma-cold beam" system ($\omega = k_z u + \eta$, $k_z u < \omega_-$) is $\gamma \sim \sqrt{n_{be}/n_0}$. For a small detuning near the $\omega \approx \omega_-$, the growth rate is proportional to $\sim \sqrt[3]{n_{be}/n_0}$. To obtain a normalized growth rates presented at Fig. 3, the equation (4) was solved for a small detuning by means of 500×500 iterations over ω and k near their resonant values at every time step. Thus the solution of Eqs.(3) and (5) are very sensitive to small variations of the ionospheric parameters the data of which are supplied in real-time mode to the input of the numerical algorithm to calculate the parameters of instabilities. To describe the instability development, the different beam-plasma models have been compared in [1]. The most satisfactory results with experimental data are obtained for the model "cold plasma-oscillator flow" in which beam particles have the finite Larmor radius and large velocity spread along the magnetic field. Despite the e_{hf} -disturbances recorded on the subsatellite may be caused by complicated plasma instabilities, the dependence of e_{hf} on ionospheric parameters due to the BPI development is evident.

At the bottom panel of Fig. 3, the spline of e_{hf} -pulsations (Bezier curve) is presented for the frequency 0.35 mHz ($\omega \sim \omega_-$). Trend e_{hf}^0 may be interpreted as VLF modulation of the HF electric field fluctuations registered by the dipole antenna at the subsatellite *Magion-3*. It is easy to see the periodic changes of the amplitude e_{hf}^0 in accordance with the three-wave resonance conditions. This effect seems to have an occasional character. But after that the HF spectra were obtained for different parameter values p (similar to that presented for ULF spectra at Fig. 4), the nonlinear wave coupling is more realizable mechanism during beams injection in the ionospheric plasma. Figures 5 and 6 present the HF spectra in the frequency range 0.01-4mHz for different values p . Spectra (a) (Fig. 5) and (c) (Fig. 5) correspond to the maximum of wave spectra energy in a resonance frequency region while the plots presented at (b) (Fig. 5) and (d) (Fig. 5) demonstrate more suppressed HF spectra. The plots sequence (a,b,c,d) is approximately in accordance with the e_{hf}^0 -behavior as a function of the parameter p . Of course, these results have to be confirmed for another ionospheric conditions and demand more complete experimental data. In spite of these effects are obtained in result of the computational experiment the input data of which consist of the active experiment measurements and simulation, the data at Figures 3-6 can be considered as an evidence of the nonlinear beating waves existence during the beam-into-beam injection.

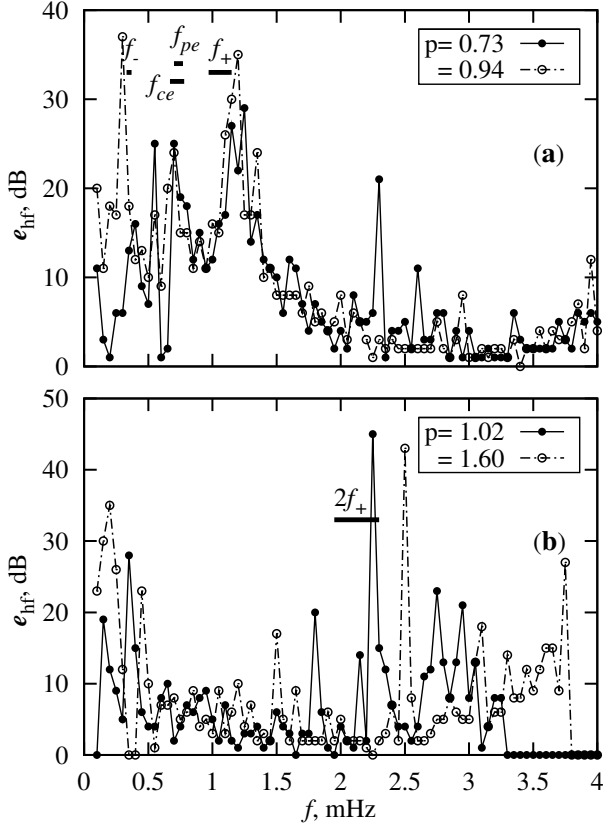


Fig. 5 HF spectra of the received signal at the *Magion-3* in the frequency range 0.1-4.0mHz for different values of the parameter p . Heavy solid segments indicate the hybrid ($\theta \sim 0.64$), electron cyclotron, and plasma frequencies f_{\pm} , f_{ce} , and f_{pe} , respectively, (here $f = \omega/2\pi$).

5. Summary

Some of these experimental results allow to assume that the excitation of lower hybrid waves leads to some electromagnetic structure which is capable to cause the beam electron oscillations and, thereby, to modulate the HF spectra at resonance frequencies. The question which effects can be observed if the satellite velocity is aligned with the magnetic field lies out of the scope of this paper. Briefly, the main results obtained during the oblique electron beam injection through the xenon ion beam can be expressed by the following.

Temporal behavior of the magnetic component amplification of VLF waves ($\sim 9 - 10$ kHz), and a satellite body potential are governed by the xenon ion beam injected into outer space simultaneously with electron beam. No beam-plasma discharges during electron beam injection from the main satellite were observed. During experiment at *Interkosmos-25*, strong negative pulses of the potential body was observed during dc-injection of the electron beam.

Current modulation in the electron gun chamber generates the beam waves with the modulation frequency ω_m . Nonlinear coupling of the waves as-

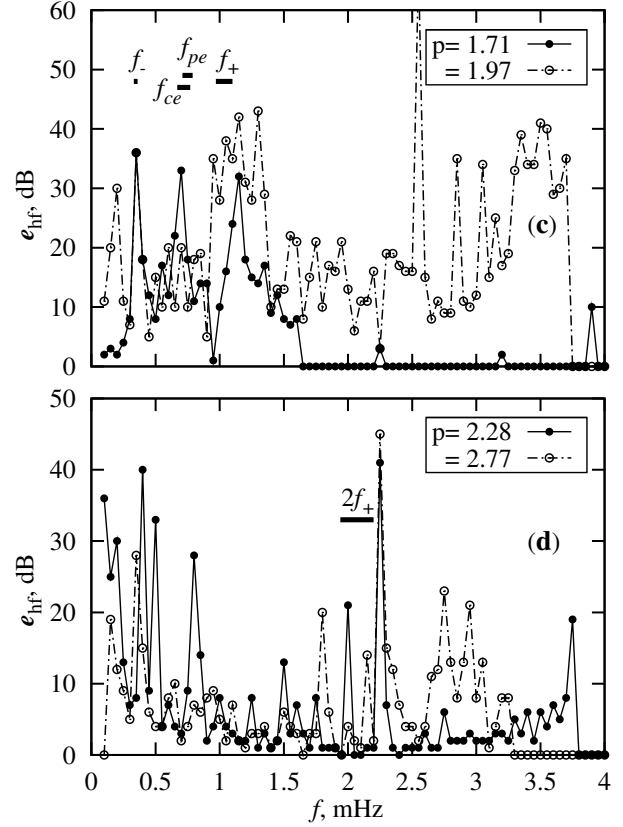


Fig. 6 HF spectra recorded at the *Magion-3* for different values of the parameter p .

sociated with the modulation frequency and slow space-charge beam waves leads to the resonant effect at the lower-hybrid frequency ω_{LH} . Most intensive ELF-ULF wave excitation was observed when the triplet wave frequencies correspond to the relationship $|\omega_m - \omega_{be}|/\omega_{LH} \sim 1$.

For the electron beam injection through an ion beam in the regime of modulation, the beating wave mode arises due to three-wave coupling at the frequencies multiple to a lower-hybrid frequency ω_{LH} . Low-frequency component of the HF electric field fluctuations is registered at *Magion-3* subsatellite. HF spectra are also varied in accordance with the three-wave frequency relationship of $\omega_m, \omega_{be}, \omega_{LH}$.

The authors would like to thank Prof. Z. Klos, Dr. M. Ciobanu, and Dr. K. Kudela for their useful discussions and support during preparing of this work.

- [1] N. V. Baranets, Ya. P. Sobolev, M. Ciobanu, et.al. *Plasma Phys. Rep.* **33**, 995 (2007).
- [2] A. B. Kitsenko, and K. N. Stepanov. *Ukr. Fiz. Zh.* **6**, 297, (1961).
- [3] V. N. Oraevskiy, Ya. P. Sobolev, L. N. Zhuzgov, et.al. *Plasma Phys. Rep.* **17**, 699 (2001).
- [4] M. M. Shoucri, G. J. Morales, and J. E. Maggs. *Phys. Fluids.* **25**, 1824 (1982).
- [5] *Radiophysical Electronics*. Ed. by N. A. Kaptsov (Mir, Moscow, 1978) [In Russian].
- [6] *Theory of plasma instabilities. V.1*. Ed. by A. B. Mikhailovskiy (Atomizdat, 1975) [In Russian].